

Electronic Structure of Silicon Nanocrystals Passivated with Nitrogen and Chlorine

Ana Martínez, Juan C. Alonso,* Luis E. Sansores, and Roberto Salcedo

Instituto de Investigaciones en Materiales, Universidad Nacional Autónoma de México,
70-360, Coyoacán 04510, D.F., México

Received: March 5, 2010; Revised Manuscript Received: June 10, 2010

The electronic structure of small (~ 1 nm) silicon nanocrystals passivated with nitrogen and chlorine is explored using density functional theory calculations. The HOMO–LUMO gap of 3.2 and 3.3 eV, calculated for the fully nitrogen [$\text{Si}_{35}(\text{NH}_2)_{36}$] and chlorine passivated ($\text{Si}_{35}\text{Cl}_{36}$) nanocrystals, respectively, correlate quite well with experimental observations describing the blue and/or white photoluminescence and electroluminescence of silicon nanocrystals, embedded in chlorinated silicon nitride films. On the other hand, the ionization energy and the electron affinity allow us to study the electron transfer properties of these systems. The charge-transfer capacity of these nanocrystals is modified in opposite directions with respect to hydrogen-passivated nanocrystals, becoming good electron acceptors with Cl passivation and good electron donors with NH_2 passivation.

I. Introduction

The study and control of the electronic structure of silicon nanocrystals (Si-nc) embedded in different silicon-based dielectric matrices has become very important for the development of low-cost optoelectronic devices. Some theoretical and experimental works indicate that the energy and efficiency of the photoluminescent emission of the Si-nc can be controlled by reducing their size, according to the quantum confinement effect.^{1–3} However, other experimental works show that the color and efficiency of their luminescent emission depends on the passivation of the surface of the Si-nc.^{4–11} For instance, in the case of Si-nc embedded in silicon dioxide thin films, which are expected to be mainly passivated with O atoms, photoluminescence is typically limited to a near-infrared and red region (1.4–1.8 eV or 886–689 nm).^{4,5} In the case of Si-nc embedded in hydrogenated silicon nitride thin films, intense visible emission from infrared (1.38 eV) to blue-violet (3.02 eV) can be obtained, depending on the growth and/or postdeposition conditions.^{2–4,6,7} In spite of this, in this case it is not clear whether the ability of the as-deposited films to emit blue light is due to N or H passivation of the Si-nc surface, and this issue is still subject to speculation and controversy.^{3,4,6,7} Si-nc embedded in chlorinated silicon nitride thin films have also been shown to have efficient photoluminescence in the red (1.8 eV) to blue-violet (3.1 eV) region, and this even improves with thermal annealing.^{8,12–14} Although in this case the Si-nc can be passivated with H, N, or Cl atoms, it has been previously speculated that their good photoluminescent properties are due to the passivation with N and/or Cl.^{12,13} However, theoretical calculations are required to support the validity of this hypothesis.

Most of the theoretical studies used to explain the experimental results on the photoluminescent properties of silicon nanoclusters embedded in thin films or in porous silicon are based on the calculation of the electronic structure and optical properties of silicon nanoclusters in vacuum and with atomic hydrogen as the main surface passivant.^{15–26} These theoretical works have shown that when the surface of Si-nc is completely passivated with hydrogen, the HOMO–LUMO gap increases

in conformity with the quantum confinement effect, and consequently, their photoluminescence can be tuned from near-infrared to ultraviolet by decreasing the size of the nanoclusters. Some calculations made for small (~ 1 nm), fully hydrogenated Si-nc, such as $\text{Si}_{35}\text{H}_{36}$, have indicated that the HOMO–LUMO gap decreases significantly when the H atoms of the Si-nc surface are partially replaced with double bonded O to form $\text{Si}_{35}\text{H}_{34}\text{O}^{20–22}$ or totally replaced with OH groups to form $\text{Si}_{35}(\text{OH})_{36}$.²³ In the first case, the HOMO–LUMO gap decreased from 3.4 eV for the $\text{Si}_{35}\text{H}_{36}$ nanocrystal to 2.1–2.2 eV for $\text{Si}_{35}\text{H}_{34}\text{O}$, and on the basis of these results, the authors explained why the upper limit of the emission energy of Si-nc passivated with oxygen is 2.1 eV (orange-red), independent of the size of the system. In the latter case [$\text{Si}_{35}(\text{OH})_{36}$] the HOMO–LUMO gap was reduced from 5.0 eV for the $\text{Si}_{35}\text{H}_{36}$ nanocrystal to 2.73 eV for $\text{Si}_{35}(\text{OH})_{36}$. These results were used to explain why hydrogen-passivated Si-nc luminesce in the blue, whereas oxide-passivated Si-nc luminesce in the red.²³ Some of these studies have also found that single-bonded surface passivators such as Cl, F, or OH produce a small variation, of 0.1 to 0.2 eV, in the HOMO–LUMO band gap of these small Si-nc.²² Recently, first-principle simulations have been made indicating that one N atom bonded to the surface of Si nanocrystals changes their HOMO–LUMO gap and plays a crucial role in defining their light emission, depending on how the N atom is bonded.²⁴ The importance of surface ligands on the electronic structure and optical response of nanoclusters has also been demonstrated recently for other semiconductors.²⁷ However, to date, there are no calculations for the HOMO–LUMO energy gap or other electronic properties of Si-nc, fully passivated with nitrogen or chlorine shells.

In this paper, a theoretical study of small silicon nanoclusters completely passivated with N and Cl is presented. The influence of the passivation on the HOMO–LUMO gap of these systems is described, in order to explain why Si-nc embedded in chlorinated silicon nitride thin films have strong blue and white photoluminescence^{12,13} and electroluminescence.²⁸ A comparative study of the electronic structure of silicon nanocrystals with sizes equal to or smaller than 1 nm whose surfaces are completely passivated with H, Cl, or N [Si_xL_y (L = H, Cl, NH_2 ;

* Corresponding author. E-mail: alonso@servidor.unam.mx.

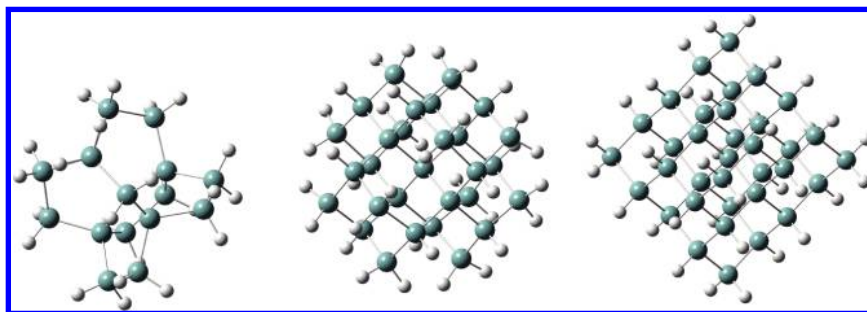


Figure 1. Optimized structures for $\text{Si}_{17}\text{H}_{24}$, $\text{Si}_{29}\text{H}_{36}$, and $\text{Si}_{35}\text{H}_{36}$.

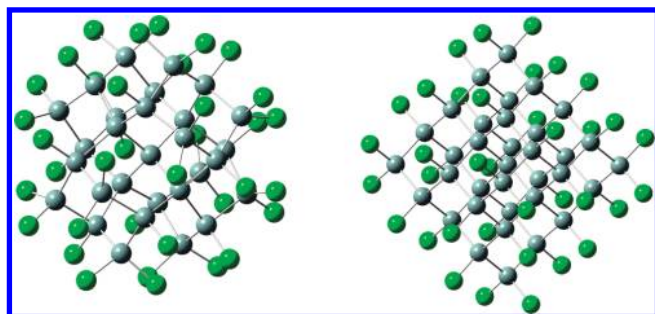


Figure 2. Optimized geometries for Si_xCl_y ($x = 29$ or 35 , $y = 36$).

$x = 17, 29, 35$; $y = 24, 36$] is included. On the other hand, the charge transfer capacity of these nanocrystals, with and without passivation, is very important and could be useful in the future to explain in more detail the electroluminescence process. For this reason, the electron donor–acceptor properties of these systems are also analyzed by calculating the ionization energy and the electron affinity. The main object of this investigation is to explore the influence of the system's size and the substitution effect on two properties: the photoluminescence and the charge transfer process.

II. Methods

Density functional approximation²⁹ as implemented in Gaussian 03³⁰ was used for all the calculations. Becke's 1988 functional, which includes the Slater exchange along with corrections involving the gradient of the density³¹ and Perdew and Wang's 1991 gradient-corrected correlation functional³² [6-31G(d,p) basis set³³] were employed in the calculations for complete optimizations, without symmetry constraints. Initial geometry for all Si_xL_y structures has T_d symmetry. For the vertical ionization energy (I) and the electron affinity (A), single-point calculations of the ions were performed at the same level of calculation as the optimized geometry of the neutrals.

In Figure 1, the optimized structures for $\text{Si}_{17}\text{H}_{24}$, $\text{Si}_{29}\text{H}_{36}$, and $\text{Si}_{35}\text{H}_{36}$ are reported. Evidently, they are highly symmetric with the terminal silicon atoms bonded to one or two hydrogen atoms. Figures 2 and 3 show the optimized geometries for Si_xCl_y and $\text{Si}_x(\text{NH}_2)_y$ ($x = 29$ or 35 , $y = 36$). These structures are slightly distorted when compared to the equivalent Si_xH_y structures. The distortion (due to the presence of the electrostatic repulsion between the chlorine atoms and the steric effects of the NH_2 substituent) is minor and the symmetry of the Si structure is almost preserved. However, the effect on the electronic properties is significant, as it can be seen with the results presented here.

III. Results and Discussion

Table 1 shows the electronic properties of structurally optimized silicon nanoclusters. It is possible to analyze the

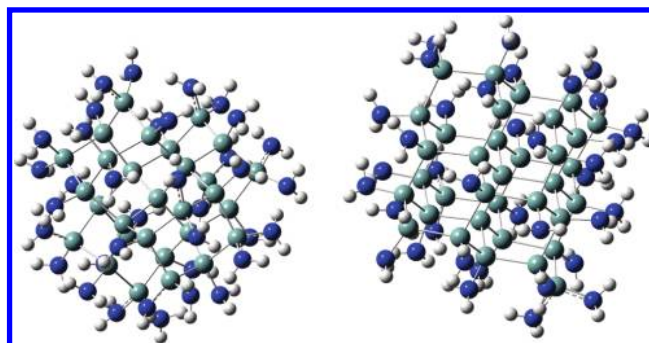


Figure 3. Optimized geometries for $\text{Si}_x(\text{NH}_2)_y$ ($x = 29$ or 35 , $y = 36$).

passivation and the size effects on the results reported in this table. With respect to the passivation effects, the $\text{Si}_{35}\text{H}_{36}$ nanocrystal has a HOMO–LUMO gap of 5.1 eV, which conforms well to previous²³ accurate calculations of the optical gap for the same nanocrystal. When the Si nanocrystal is completely passivated with Cl or NH_2 , the gap drops to values of 3.3 and 3.2 eV, for $\text{Si}_{35}\text{Cl}_{36}$ and $\text{Si}_{35}(\text{NH}_2)_{36}$, respectively. This reduction of the HOMO–LUMO gap is similar to that reported previously²² when H was replaced by OH groups to form $\text{Si}_{35}(\text{OH})_{36}$ (gap is equal to 2.7 eV). However, nanocrystals passivated with chlorine or nitrogen manifest a smaller gap reduction than when the system is passivated with OH, and these gaps are great enough (3.2–3.3 eV) to have an upper limit that explains the light emission energy in the blue and even in the violet region.

With respect to the size effects, the data presented in Table 1 indicate that the HOMO–LUMO gap of the hydrogen-passivated nanocrystal follows the trend displayed in quantum confinement models, as the band gap increases as the diameter decreases. It registers as 5.1, 5.2, and 5.6 eV for $\text{Si}_{35}\text{H}_{36}$, $\text{Si}_{29}\text{H}_{36}$, and $\text{Si}_{17}\text{H}_{24}$, respectively. It is possible to observe the same quantum confinement effect in the nanocrystals passivated with chlorine, since the gaps of $\text{Si}_{35}\text{Cl}_{36}$ and $\text{Si}_{29}\text{Cl}_{36}$ are 3.3 and 3.6 eV, respectively. However, this effect is not observed in the case of NH_2 passivation. In this case, the HOMO–LUMO gap is 3.2 eV for both systems $\text{Si}_{36}(\text{NH}_2)_{36}$ and $\text{Si}_{29}(\text{NH}_2)_{36}$. It is important to note that the HOMO–LUMO band gap increases as the diameter decreases, mainly due to the destabilization of the HOMO and the stabilization of the LUMO. The present results in silicon hydrides do not show a trend in the LUMO energies or electron affinities versus size. Nevertheless, the HOMO and LUMO energies show clear tendency that depend on chemical substitution, as can be seen in Table 1 and in what follows.

On the basis of these results, concerning the size and substituent effects on the HOMO–LUMO gap, the strong white and blue photoluminescence experimentally observed in Si-nc

TABLE 1: Properties of the Optimized Structures (in eV)

	Si ₁₇ H ₂₄	Si ₂₉ H ₃₆	Si ₃₅ H ₃₆	Si ₂₉ Cl ₃₆	Si ₃₅ Cl ₃₆	Si ₂₉ (NH ₂) ₃₆	Si ₃₅ (NH ₂) ₃₆
HOMO	-7.2	-6.9	-6.8	-7.8	-7.7	-4.3	-4.4
LUMO	-1.6	-1.7	-1.7	-4.2	-4.4	-1.1	-1.2
LUMO-HOMO gap	5.6	5.2	5.1	3.6	3.3	3.2	3.2
vertical ionization energy (<i>I</i>)	8.3	7.9	7.7	8.6	8.6	5.2	5.3
vertical electron affinity (<i>A</i>)	0.8	0.7	0.8	3.4	3.6	0.2	0.4
Fermi energy	-4.5	-4.3	-4.3	-6.0	-6.1	-2.7	-2.9
hardness (<i>I</i> - <i>A</i>)	7.5	7.2	6.9	5.2	5.0	5.0	4.9
ω^- (electrodonating) ^a	5.5	5.2	5.2	10.3	10.8	3.1	3.4
ω^+ (electroaccepting) ^b	0.9	0.9	0.9	4.3	4.7	0.4	0.5

^a Lower values of electrodonating power imply a greater capacity for donating charge. ^b Higher values of electroaccepting power imply a greater capacity for accepting charge.

embedded in chlorinated silicon nitride thin films,^{12,13} can be explained as follows. Since these films have Si-nc with diameters of 0.7–4 nm,^{13,14} the emission of the smaller Si-nc (0.7–1 nm) will be evidently in the blue-violet region, no matter if they are completely passivated by nitrogen, chlorine, or hydrogen, because they have a HOMO–LUMO gap equal to 3.2–5.6 eV. On the other hand, since the HOMO–LUMO gap of Si-nc completely passivated with hydrogen or chlorine is reduced as their size increases, the larger ones (3–4 nm) will emit in the red and/or infrared region. According to our results, the smaller (~1 nm) Si-nc completely passivated with nitrogen will emit in the blue region (3.2 eV). Thus, depending on the distribution of sizes and the density of Si-nc passivated with hydrogen, chlorine, or nitrogen, the total photoluminescence may be either white or blue. In previous work, Dal Negro et al.²⁴ reported the role of N atoms bonded to the surface of Si clusters in the emission mechanism. They reported the HOMO–LUMO gap for partially nitrogen-passivated nanocrystals, calculated within the local density approximation. The HOMO–LUMO gap that we report in Table 1 was obtained for fully nitrogen passivated nanocrystals, calculated with the gradient-corrected correlation functional. It is not feasible to compare directly our results with those obtained for partially nitrogen-passivated nanocrystals, because the latter were calculated using DFT within the local density approximation (LDA), which underestimates the true optical gaps.²⁴ However, it is possible to say that we reach the same conclusion in terms of the effect of nitrogen passivation on the emission properties of the Si-nc, since in that case the addition of one N atom also lowers the calculated gaps with respect to the Si₃₅H₃₆ nanocrystal.²⁴

As can be observed in Table 1, compared with Si₃₅H₃₆, chlorine drastically stabilized the LUMO, whereas passivation with NH₂ significantly destabilized the HOMO. This is consistent with the fact that chlorine is an electron acceptor, whereas NH₂ is an electron donor and consequently they both modified the ionization energy and the electron affinity of the systems. Substituents effects on the HOMOs and LUMOs are presented graphically in Figures 1S and 2S of the Supporting Information. HOMOs and LUMOs are mainly π bonding orbitals and their localization is the principal difference among the systems. As can be seen with these figures and the values reported in Table 1, the energy shifts are not related to trends in the amplitudes of the orbitals. The orbitals of Si_xH_y are symmetrically distributed, while it is not the case for Si_xCl_y and Si_x(NH₂)_y. The substitution affects the localization of the orbitals in such a way that HOMOs are located mostly on the outer atoms of the system and LUMOs are localized on the inner shell of the atoms.

Table 1 shows the results of the vertical ionization energy (*I*) and vertical electron affinity (*A*), obtained from the single-point energy calculations of the neutral optimized structures. As can be seen, in both cases (with Cl and NH₂) the

HOMO–LUMO gap is similar and smaller than that of Si_xH_y. However, electronegative chlorine decreases the energy of both the HOMO and LUMO, and the electron affinity of the systems increased considerably. NH₂ also affects HOMO and LUMO (both show an increase in energy) and the ionization potential is decreased slightly. As shown in Table 1, Si_x(NH₂)_y has the lowest ionization energy and Si_xCl_y the highest electron affinity, and consequently, Si_xH_y, Si_xCl_y, and Si_x(NH₂)_y species have very different values in terms of their Fermi energy, $-(I + A)/2$, the lowest being those systems passivated with NH₂ and the highest, those systems passivated with Cl. The Fermi level becomes more negative with chlorine because the electron affinity is higher. In contrast, the Fermi energy is less negative with NH₂. The electron-transfer hardness (*I* - *A*) decreases by 2.2 eV when H atoms are substituted with either Cl or with NH₂. Since hardness assesses resistance to the electron flow, it is possible to deduce that Si_xH_y will have the greatest resistance to the electron flow out of all the systems in the study.

A useful way of measuring electrodonating and electroaccepting power was recently described by Gázquez et al.³⁴ They established a simple charge-transfer model and analyzed the global response of a molecule immersed in an idealized environment that may either withdraw or donate charge. An alternative quadratic interpolation for the energy as a function of the number of electrons was proposed, in order to evaluate the response of a molecule to charge acceptance or withdrawal, in terms of its electron affinity and ionization potential. Referring to this approximation, these authors conclude that the propensity to donate charge, or electrodonating power, may be defined as

$$\omega^- = \frac{(3I + A)^2}{16(I - A)} \quad (1)$$

whereas the propensity to accept charge, or electroaccepting power, may be defined as

$$\omega^+ = \frac{(I + 3A)^2}{16(I - A)} \quad (2)$$

In the case of electrodonating power, lower values imply a greater capacity for donating charge. In the case of electroaccepting power, higher values imply a greater capacity for accepting charge. It is important to note that *I* and *A* refer to donating or accepting a single, whole electron, whereas ω^- and ω^+ refer to fractional charges. In this way, the electrodonating and electroaccepting powers are based on a simple charge transfer model, expressed in terms of chemical potential and hardness. Electrodonating power ascribes more emphasis to ionization potential than to electron affinity in the context of the charge donation process. Contrarily,

electroaccepting power assigns more significance to electron affinity than to ionization potential.

As can be observed in Table 1, in the case of electroaccepting and electrodonating powers, size is less important than the substituent effect. Si_xCl_y system is the best electron acceptor and the worse electron donor, whereas the $\text{Si}_x(\text{NH}_2)_y$ system is the best electron donor and the worst electron acceptor. For Si_xCl_y , the bigger system is a better electron acceptor compared to the small one, whereas for Si_xH_y and $\text{Si}_x(\text{NH}_2)_y$ the electron donor–acceptor capacity is less affected by the size of the system. These results can help to explain in more detail the electroluminescence of silicon nanocrystals, embedded in chlorinated silicon nitride films.²⁸

IV. Conclusions

In conclusion, we have found that the HOMO–LUMO gap is smaller for big systems than for the small ones, but the influence of the system's size is less important than the substitution effect. The HOMO–LUMO gap is almost 2 eV smaller for the chlorine- or nitrogen-passivated systems than for Si_xH_y , and is practically the same for Si_xCl_y as it is for $\text{Si}_x(\text{NH}_2)_y$. The values of the HOMO–LUMO gap of 3.2 and 3.3 eV, calculated for the fully nitrogen-passivated $[\text{Si}_{35}(\text{NH}_2)_{36}]$ and chlorine-passivated ($\text{Si}_{35}\text{Cl}_{36}$) nanocrystals, respectively, correlate well with the white and blue photoluminescence of silicon nanocrystals, embedded in chlorinated silicon nitride films. Our results also show that the charge-transfer capacity is drastically modified with the passivation of the system but in opposite directions, i.e., with Cl it will become a good electron acceptor, whereas with NH_2 it will become a good electron donor. This study is important because it gives knowledge to control the photoluminescent and electroluminescent properties of silicon nanocrystals embedded in different silicon-based dielectric matrices, and this could be useful for the development of low-cost optoelectronic devices.

Acknowledgment. This study was made possible due to funding from the Consejo Nacional de Ciencia y Tecnología (CONACyT), as well as resources provided by the Instituto de Investigaciones en Materiales IIM, UNAM. The work was carried out, using a KanBalam supercomputer, provided by DGSCA, UNAM, and the facilities at Laboratorio de Supercomputo y Visualización en Paralelo de UAM Iztapalapa. The authors would like to acknowledge both Oralia L. Jiménez A and María Teresa Vázquez for their technical support. We would also like to thank Caroline Karlake (Master's, Social Anthropology, Cambridge University, England) for reviewing the manuscript for grammar and style.

Supporting Information Available: Molecular orbital pictures (Figures 1S and 2S). This material is available free of charge via Internet at <http://pubs.acs.org>.

References and Notes

- (1) Takagahara, T.; Takeda, K. Theory of the Quantum Confinement Effect on Excitons in Quantum of Indirect-Gap Materials. *Phys. Rev. B* **1992**, *46*, 15578.
- (2) Kim, T. Y.; Park, N. M.; Kim, K. H.; Sung, G. Y.; Ok, Y. W.; Seong, T. Y.; Choi, C. J. Quantum Confinement Effect of Silicon Nanocrystals in-Situ Grown in Silicon Nitride Films. *Appl. Phys. Lett.* **2004**, *85*, 5355.
- (3) Kim, T. W.; Cho, C. H.; Kim, B. H.; Park, S. J. Quantum Confinement Effect of Crystalline Silicon Quantum Dots in Silicon Nitride Grown Using SiH_4 and NH_3 . *Appl. Phys. Lett.* **2006**, *88*, 123102.
- (4) Yang, M. S.; Cho, K. S.; Jhe, J. H.; Seo, S. Y.; Shin, J. H.; Kim, K. J.; Moon, D. W. Effect of Nitride Passivation on the Visible Photoluminescence from Silicon Nanocrystals. *Appl. Phys. Lett.* **2004**, *85*, 3408.
- (5) Cao, Z. X.; Song, R.; Ma, L. B.; Du, Y.; Ji, A. L.; Wang, Y. Q. Visible Light Emission from Innate Silicon Nanocrystals in an Oxide Matrix Grown at Low Temperature. *Nanotechnology* **2006**, *17*, 2073.
- (6) Kim, B. H.; Cho, C. H.; Kim, T. W.; Park, N. M.; Sung, G. Y.; Park, S. Photoluminescence of Silicon Quantum Dots in Silicon Nitride Grown by NH_3 and SiH_4 . *J. Appl. Phys. Lett.* **2005**, *86*, 091908.
- (7) Ma, K.; Feng, J. Y.; Zhang, Z. J. Improved Photoluminescence of Silicon Nanocrystals in Silicon Nitride Prepared by Ammonia Sputtering. *Nanotechnology* **2006**, *17*, 4650.
- (8) Santana, G.; Monroy, B. M.; Ortiz, A.; Huerta, L.; Alonso, J. C.; Fandiño, J.; Aguilar-Hernández, J.; Hoyos, E.; Cruz-Gandarilla, F.; Contreras-Puentes, G. Influence of the Surrounding Host in Obtaining Tunable and Strong Visible Photoluminescence from Silicon Nanoparticles. *Appl. Phys. Lett.* **2006**, *88*, 041916.
- (9) Godefroo, S.; Hayne, M.; Jivanescu, M.; Stesmans, A.; Zacharias, M.; Lebedev, O. I.; Van Tendeloo, G.; Moshchalkov, V. V. Classification and Control of the Origin Photoluminescence from Si Nanocrystals. *Nat. Nanotechnol.* **2008**, *3*, 174.
- (10) Salivati, N.; Shuall, N.; Baskin, E.; Garber, V.; McCrate, J. M.; Ekerdt, J. G. Influence of Surface Chemistry on Photoluminescence from Deuterium-Passivated Silicon Nanocrystals. *J. Appl. Phys.* **2009**, *106*, 063121.
- (11) Dobrovolskas, D.; Mickevicius, J.; Tamulaitis, G.; Reipa, V. Photoluminescence of Si Nanocrystals under Selective Excitation. *J. Phys. Chem. Sol.* **2009**, *70*, 439.
- (12) Benami, A.; Santana, G.; Ortiz, A.; Ponce, A.; Romeu, D.; Aguilar-Hernández, J.; Contreras-Puentes, G.; Alonso, J. C. Strong White and Blue Photoluminescence from Silicon Nanocrystals in SiN_x Grown by Remote PECVD Using $\text{SiCl}_4/\text{NH}_3$. *Nanotechnology* **2007**, *18*, 155704.
- (13) Benami, A.; Santana, G.; Monroy, B. M.; Ortiz, A.; Alonso, J. C.; Fandiño, J.; Aguilar-Hernández, J.; Contreras-Puentes, G. Visible Photoluminescence from Silicon Nanoclusters Embedded in Silicon Nitride Films Prepared by Remote-Plasma Enhanced Chemical Vapor Deposition. *Physica E* **2007**, *38*, 148.
- (14) Ponce, A.; Benami, A.; Santana, G.; Alonso, J. C.; Aguilar-Hernández, J.; Contreras-Puentes, G.; Ortiz, A.; Fandiño, J.; Romeu, D. Structural Evolution of Nanocrystalline Silicon Studied by High Resolution Transmission Electron Microscopy. *Phys. Stat. Solidi C* **2007**, *4*, 1458.
- (15) Wang, L.; Zunger, A. J. Electronic Structure Pseudopotential Calculations of Large (~1000 atoms) Si Quantum Dots. *Phys. Chem.* **1994**, *98*, 2158.
- (16) Allan, G.; Delerue, C.; Lannoo, M. Electronic Structure of Amorphous Silicon Nanoclusters. *Phys. Rev. Lett.* **1997**, *78*, 3161.
- (17) Ogut, S.; Chelikowsky, J. M.; Louie, S. G. Quantum Confinement and Optical Gaps in Si Nanocrystals. *Phys. Rev. Lett.* **1997**, *79*, 1770.
- (18) Rohlfing, M.; Louie, S. G. Excitonic Effects and the Optical Absorption Spectrum of Hydrogenated Si Clusters. *Phys. Rev. Lett.* **1998**, *80*, 3320.
- (19) Vasiliev, I.; Ogut, S.; Chelikowsky, J. R. Ab Initio Absorption Spectra and Optical Gaps in Nanocrystalline Silicon. *Phys. Rev. Lett.* **2001**, *86*, 1813.
- (20) Wolkin, M. V.; Jorne, J.; Fauchet, P. M.; Allan, G.; Delerue, C. Electronic States and Luminescence in Porous Silicon Quantum Dots: The Role of Oxygen. *Phys. Rev. Lett.* **1999**, *82*, 197.
- (21) Vasiliev, I.; Ogut, S.; Chelikowsky, J. R.; Martin, R. M. Surface Oxidation Effects on the Optical Properties of Silicon Nanocrystals. *Phys. Rev. B* **2002**, *65*, 121302R.
- (22) Puzder, A.; Williamson, A. J.; Grossman, J. C.; Galli, G. Surface Chemistry of Silicon Nanoclusters. *Phys. Rev. Lett.* **2002**, *88*, 097401.
- (23) Zhou, Z.; Brus, L.; Friesner, R. Electronic Structure and Luminescence of 1.1- and 1.4-nm Silicon Nanocrystals: Oxide Shell versus Hydrogen Passivation. *Nano Lett.* **2003**, *3*, 163.
- (24) Dal Negro, L.; Yi, J. H.; Kimerling, L. C.; Hamel, S.; Williamson, A.; Gali, G. Light Emission from Silicon Rich Nitride Nanostructures. *Appl. Phys. Lett.* **2006**, *88*, 183103.
- (25) Hyeon-Deuk, K.; Madrid, A. B.; Prezhdo, O. V. Symmetric Band Structures and Asymmetric Ultrafast Electron and Hole Relaxations in Silicon and Germanium Quantum Dots: Time-Domain Ab Initio Simulation. *Dalton Trans.* **2009**, *45*, 10069.
- (26) Madrid, A. B.; Hyeon-Deuk, K.; Habenicht, B. F.; Prezhdo, O. V. Phonon-Induced Dephasing of Excitons in Semiconductor Quantum Dots: Multiple Exciton Generation, Fission, and Luminescence. *ACS Nano* **2009**, *3*, 2487.
- (27) Kilina, S.; Ivanov, S.; Tretiak, S. Effect of Surface Ligands on Optical and Electronic Spectra of Semiconductor Nanoclusters. *J. Am. Chem. Soc.* **2009**, *131*, 7717.
- (28) Alonso, J. C.; Pulgarin, F. A.; Monroy, B. M.; Benami, A.; Bizarro, M.; Ortiz, A. Visible Electroluminescence from Silicon Nanoclusters Embedded in Chlorinated Silicon Nitride Thin Films. *Thin Solid Films* **2010**, *518*, 3891.
- (29) Kohn, W.; A. D. Becke, A. D.; Parr, R. G. Density Functional Theory of Electronic Structure. *J. Phys. Chem.* **1996**, *100*, 12974.

(30) Frisch, M. J.; Trucks, G. W.; Schlegel, H. B.; Scuseria, G. E.; Robb, M. A.; Cheeseman, J. R.; Montgomery, J. J. A.; Vreven, T.; Kudin, K. N.; Burant, J. C.; et al. *Gaussian 03*; Gaussian, Inc.: Wallingford CT, 2004.

(31) Becke, A. D. Density-Functional Exchange-Energy Approximation with Correct Asymptotic Behavior. *Phys. Rev. A* **1988**, *38*, 3098.

(32) (a) Perdew, J. P.; Wang, Y. Accurate and Simple Analytic Representation of the Electron-Gas Correlation Energy. *Phys Rev B* **1992**, *45*, 13244. (b) Perdew, J. P.; Burke, K.; Wang, Y. *Phys. Rev. B* **1996**, *54*, 16533. (c) Perdew, J. P. In *Electronic Structure of Solids '91*; Ziesche, P.; Eschrig, H., Eds.; Akademie Verlag, Berlin, 1991.

(33) (a) Krishnan, R.; Binkley, J. S.; Seeger, R.; Pople, J. A. Self-Consistent Molecular Orbital Methods XX. A Basis Set for Correlated Wave Functions. *J. Chem. Phys.* **1980**, *72*, 650. (b) McLean, A. D.; Chandler, G. S. *J. Chem. Phys.* **1980**, *72*, 5639. (c) Clark, T.; Chandrasekhar, J.; Spitznagel, G. W.; Schleyer, P. V. R. *J. Comput. Chem.* **1983**, *4*, 294.

(34) Gázquez, J. L.; Cedillo, A.; Vela, A. Electrodonating and Electroaccepting Powers. *J. Phys. Chem. A* **2007**, *111*, 1966.

JP102017D